Supplementary Material (ESI) for Molecular BioSystems

Evolvability and robustness in a complex signalling circuit

Supplementary material

Karthik Raman[1,2] and Andreas Wagner[1,2,3]

[1]*Department of Biochemistry, University of Zürich, Winterthurerstrasse 190, 8057 Zürich, Switzerland*
[2]*Swiss Institute of Bioinformatics, Quartier Sorge, Batiment Genopode, 1015 Lausanne, Switzerland*
[3]*The Santa Fe Institute, 1399 Hyde Park Road, Santa Fe, NM 87501, USA*

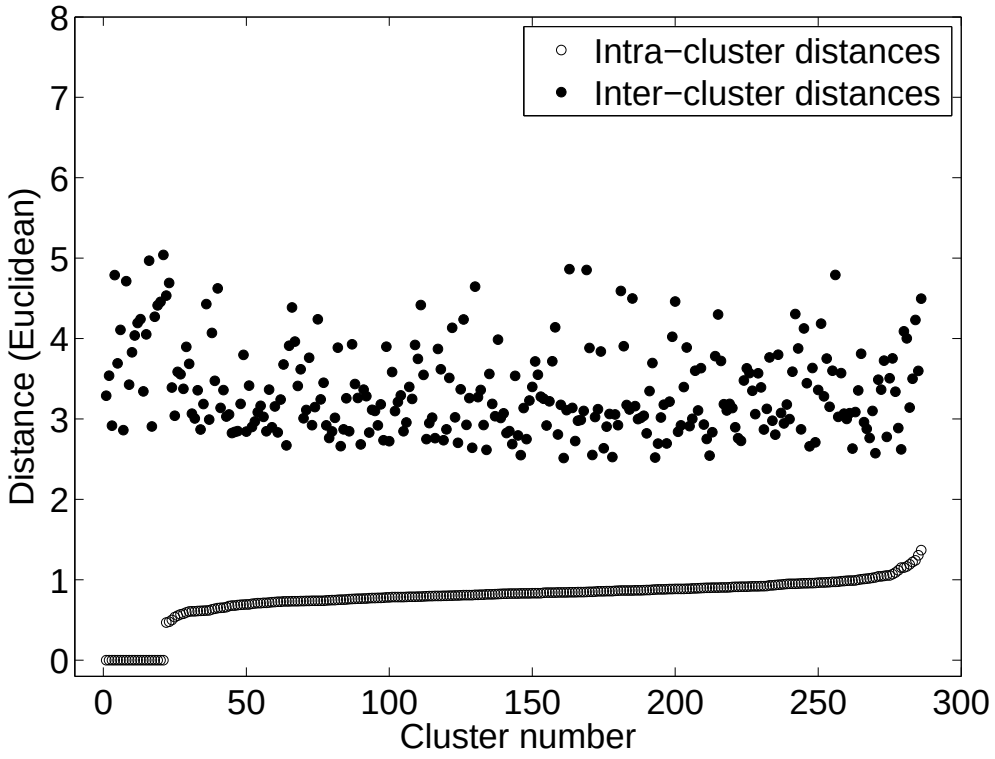

Figure S1: **Mean distance within clusters and between clusters.** The figure shows the distribution of inter-cluster distances (closed circles) and intra-cluster distances (open circles), for the 286 clusters. All distances are computed in trajectory space, using the Euclidean metric (vertical axis). The horizontal axis indicates the 286 clusters, sorted based on inter-cluster distances. For analysing intra-cluster distances, we computed pairwise distances between all the trajectories within a cluster. For analysing inter-cluster distances, we computed the distance between the centres of each of the clusters. This analysis is a rough measure of cluster quality; a higher separation between the two sets of distances is indicative of a better clustering. For our models, we can indeed see a good separation of the clusters. Error bars (for one standard error) are smaller than the symbols and hence not shown.

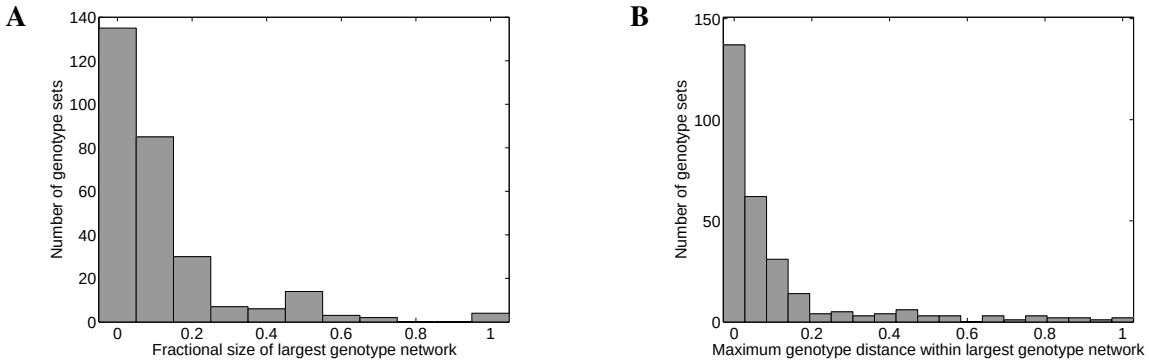

Figure S2: **(A) Distribution of the fraction of a genotype set occupied by the largest genotype network, for all genotype sets**. **(B) Distribution of maximum genotype distance within the largest genotype network of a set, for all genotype sets.** Note that the maximum genotype distance has been expressed as a fraction of genotype space diameter (18).

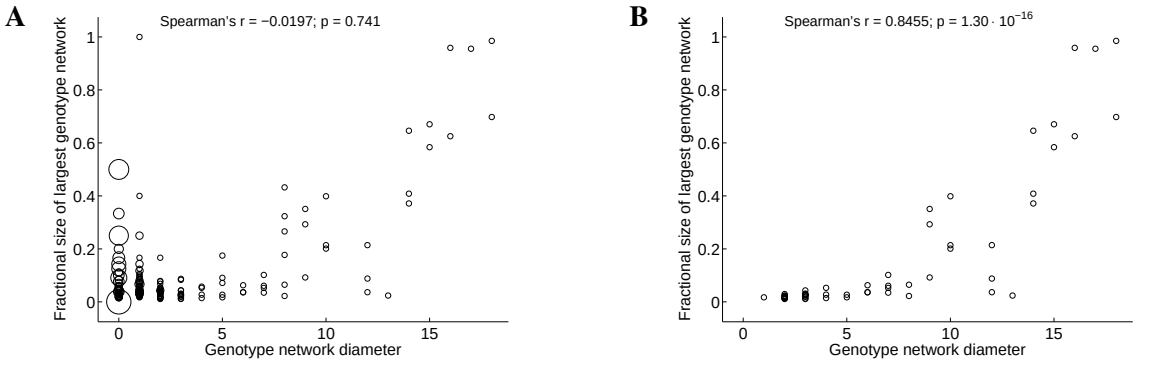

Figure S3: **Genotype networks that occupy a larger fraction of a genotype set extend further through genotype space.** (A) All genotype sets. (B) Large genotype sets.

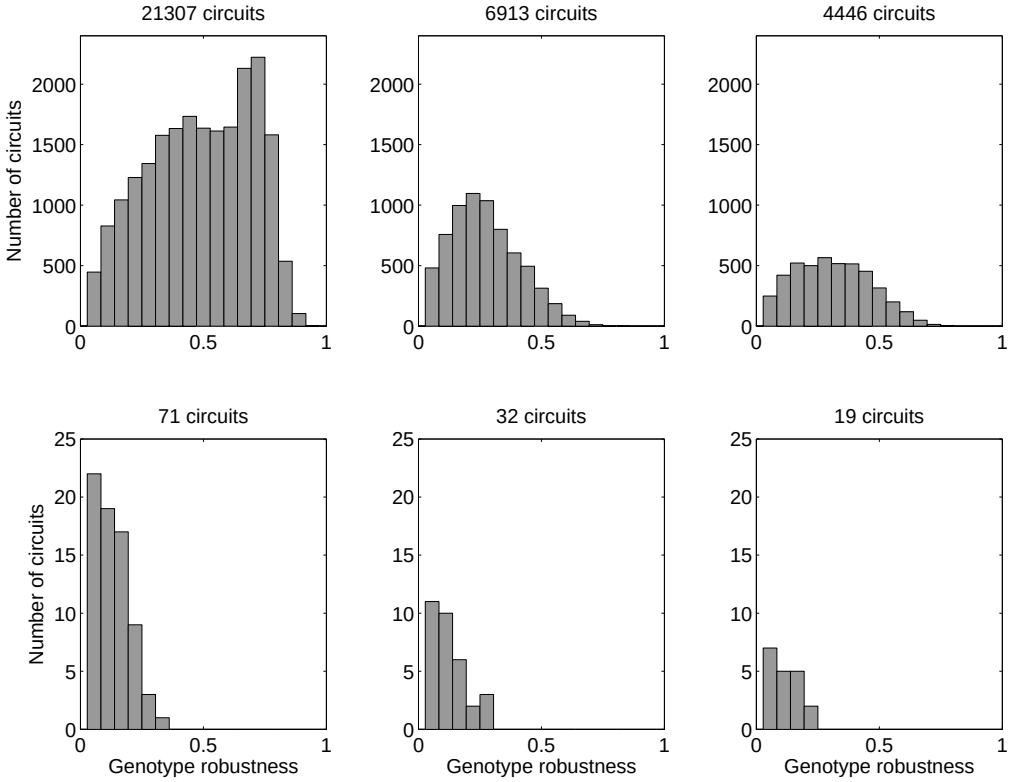

Figure S4: **Larger genotype networks contain more robust genotypes.** The top panel indicates the distribution of genotype robustness for the three largest networks. The bottom panel indicates the same distribution, but for three networks of smaller sizes. The total number of genotypes (circuits) in each network is also indicated in the plots. Note the difference in scale for the vertical axis between the top and bottom panels.

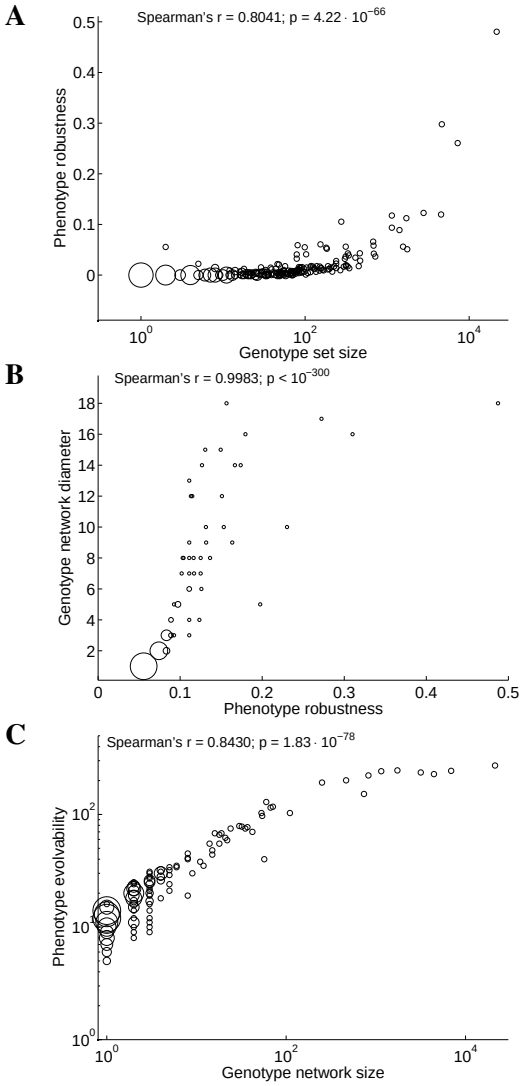

Figure S5: **(A) Phenotypes of larger genotype sets are more robust. (B) Genotype networks corresponding to robust phenotypes have greater network diameters. (C) Larger genotype networks have a greater number of phenotypes in their neighbourhood.** The panel shows the correlation between phenotype evolvability and the size of the largest genotype network, for all genotype sets.

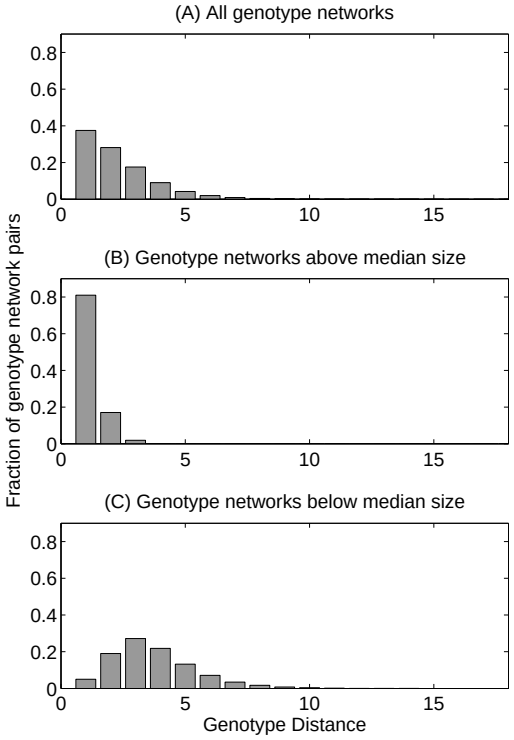

Figure S6: **Circuits with different phenotypes can be found close together in genotype space.** The figure shows the distribution of minimum genotype distance between genotype networks (A) of all sizes, (B) above median size and (C) below median size. Only the largest genotype network for each phenotype has been considered. The minimum distance between the genotype networks is computed as described in the main text. The figure shows that the distances between smaller genotype networks are larger than the distances between larger genotype networks. Thus, large genotype networks are especially close in genotype space.

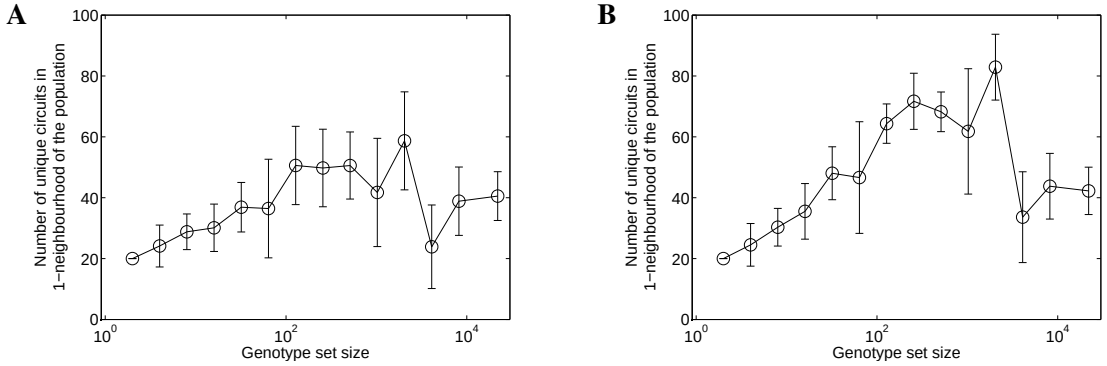

Figure S7: **Populations evolving on larger genotype networks can access more new phenotypes.** The largest genotype network from each of the large genotype sets were binned by size and the mean number of unique phenotypes in the 1-neighbourhood of the entire population (after 100 generations) has been indicated for the different bins. The error bars indicate one standard deviation. Mutation rate per generation per individual: (A) $\mu = 0.10$. (B) $\mu = 0.50$. In all cases, population size $N = 100$.

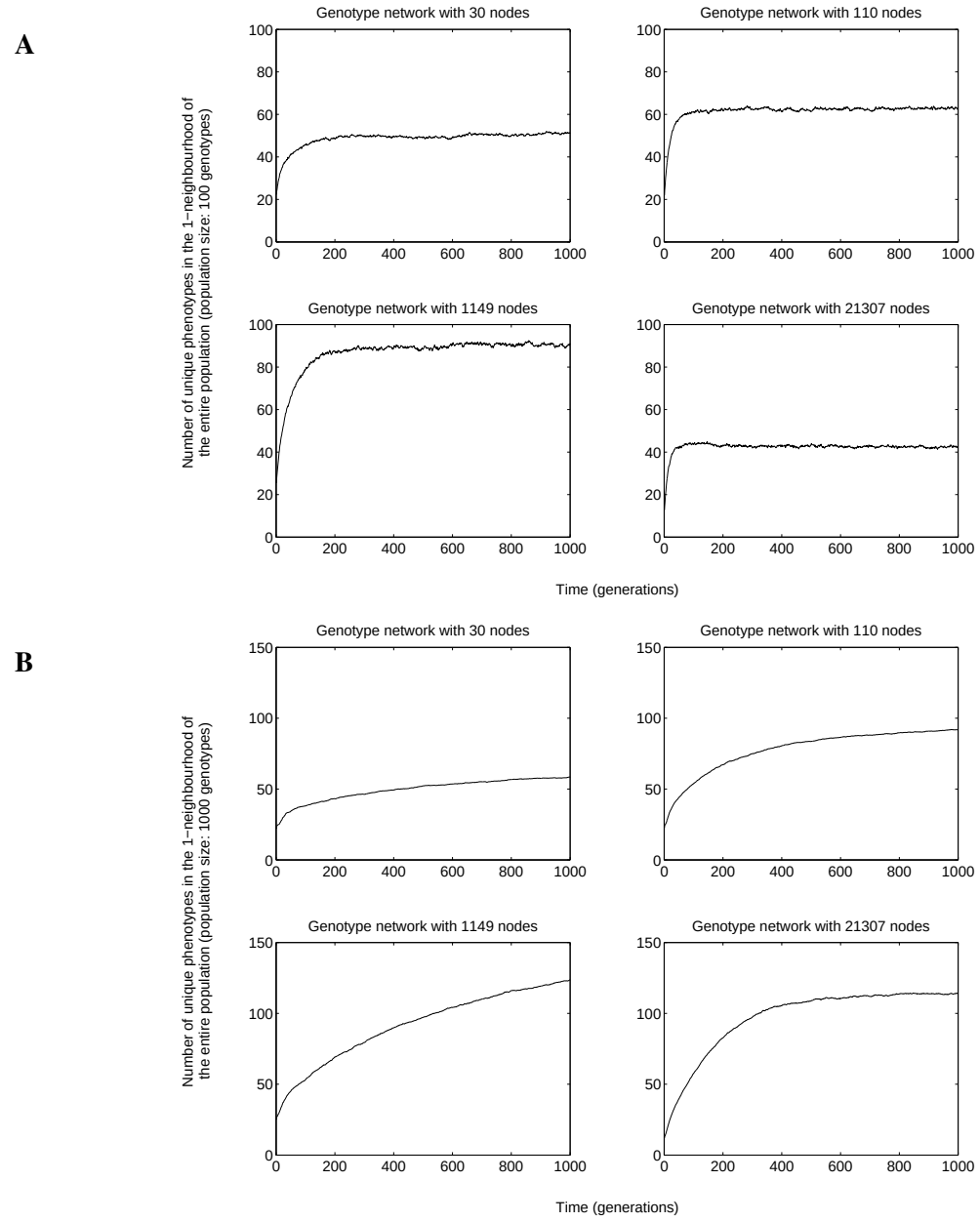

Figure S8: **Phenotypic diversity in the neighbourhood of populations evolving on different genotype networks.** The figure shows the progression with time of the number of unique phenotypes in the neighbourhood of a population evolving on a genotype network ($P_U(t)$), for population sizes of 100 (panel A) and 1000 (panel B). In the largest genotype network, many of the neighbours of a genotype have the same phenotype; thus the 1-neighbourhood contains a large fraction of genotypes with the same phenotype, and consequently fewer unique new phenotypes. For very small genotype networks, the size of network's 1-neighbourhood is smaller, and therefore the number of unique phenotypes in the neighbourhood is also lower. For networks of intermediate size (1149 nodes in this example), the number of phenotypes in the neighbourhood increases to the largest steady-state value. As one would expect, for larger population sizes (panel B), we find a greater number of unique phenotypes in a population's neighbourhood. In all panels, the mutation rate per generation per individual was $\mu = 0.25$. In both (A) and (B), we consider the same set of genotype networks, with sizes as indicated in the sub-panel headers. Note that the vertical scales are different for (A) and (B).

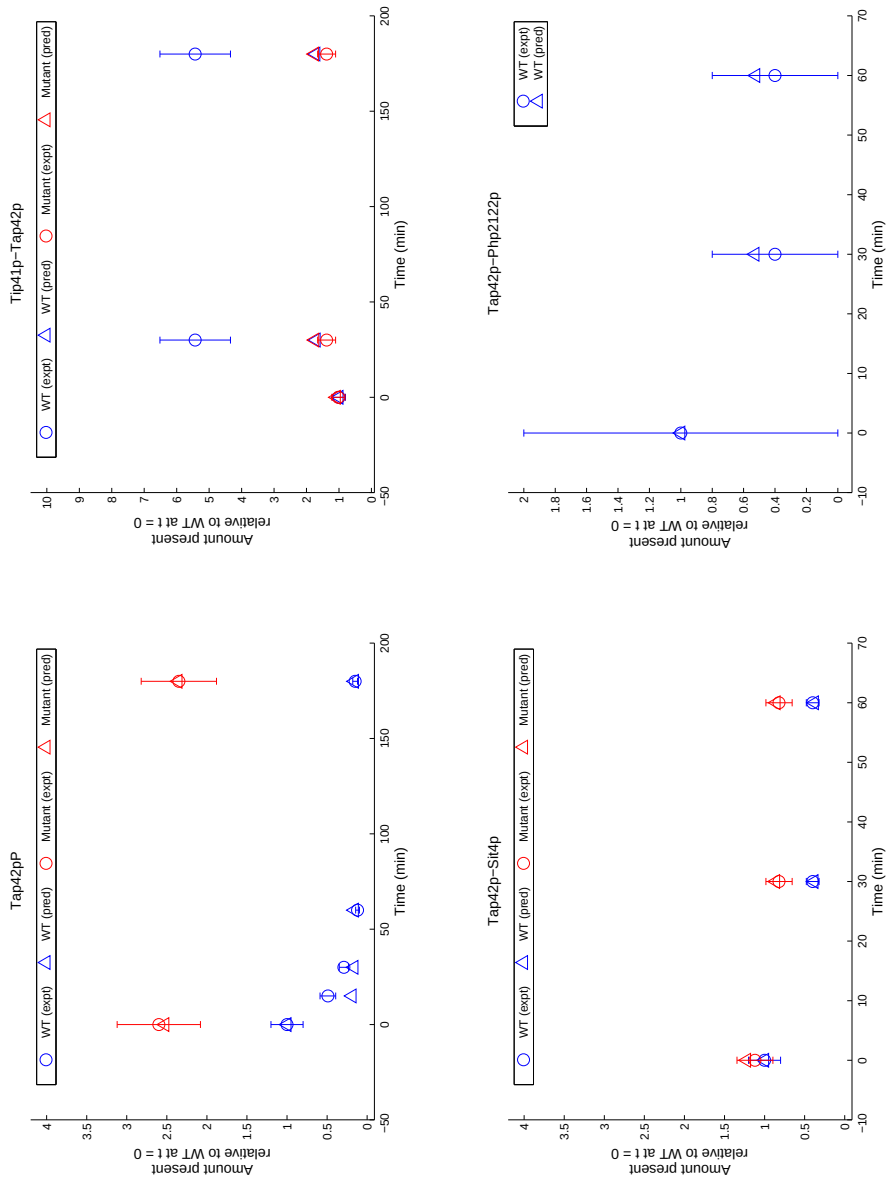

Figure S9: **Comparison of time course data and predicted time courses for some key signalling molecules and for the CORE model of the signalling pathway.** Note that the prediction of the time course for the Tip41p-Tap42p complex is rather poor. In comparison, the inclusion of Variant V_1 in the model gives much better results, as shown in Fig. S10. The experimental time course data were obtained from multiple experiments [1–5], as detailed in Table S2 and ref. 1. The error bars represent the uncertainty in the experimental data, as described in ref. 1

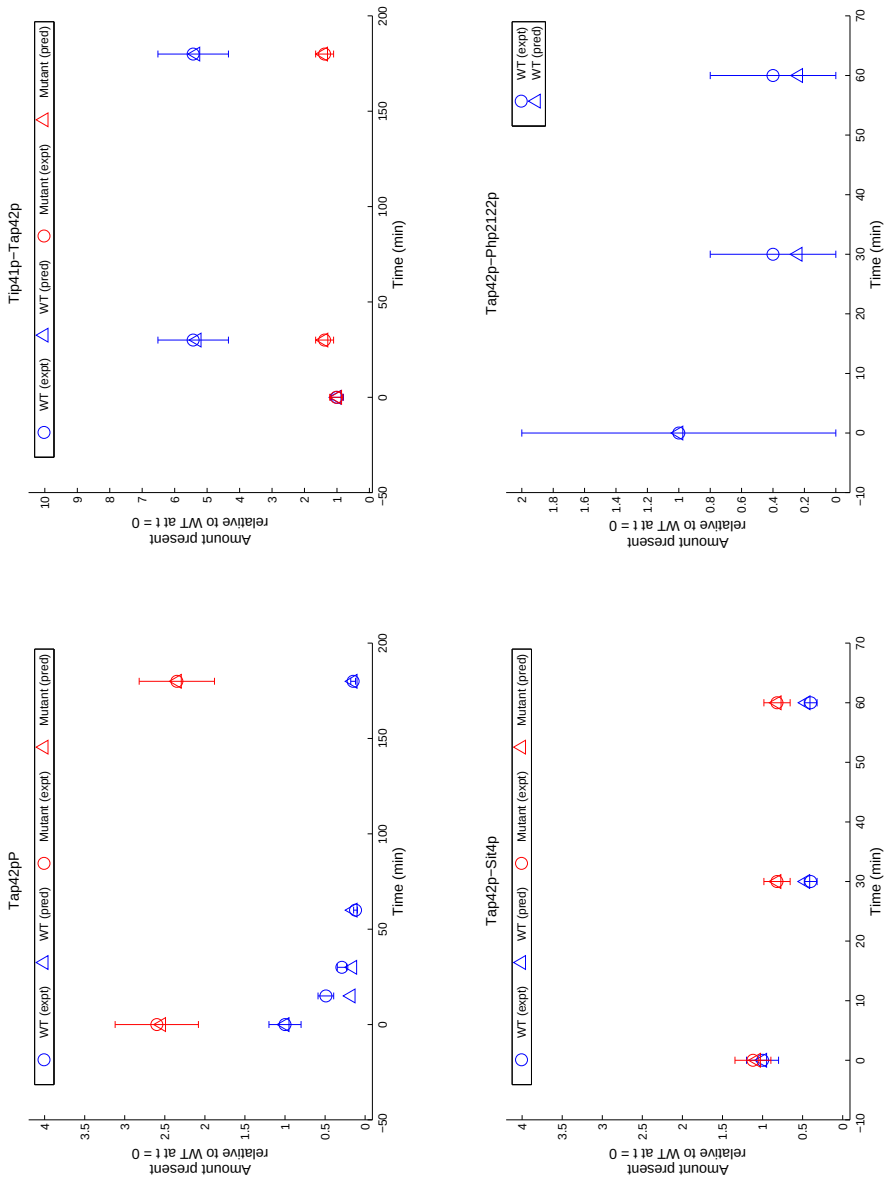

Figure S10: **Comparison of time course data and predicted time courses for some key signalling molecules.** The model is based on the CORE model, combined with variant V_1, which corresponds to the hypothesis that Tip41p has two phosphorylation sites. The experimental time course data were obtained from multiple experiments [1–5], as detailed in Table S2 and ref. 1. The error bars represent the uncertainty in the experimental data, as described in ref. 1

V_1 :	Tip41p has two phosphorylation sites
V_2 :	Tap42p$^{\textcircled{P}}$-Pph21/22p forms an anti-phosphatase protecting phosphoproteins
V_3 :	Complex formation of Tap42p$^{\textcircled{P}}$ and Tip41p
V_4 :	Complex formation of Tap42p$^{\textcircled{P}}$ and Tip41p$^{\textcircled{P}}$
V_5 :	Pph21/22p is phosphorylated by Tor1/2p and dephosphorylated by PP2A1/2
V_6 :	Tap42p$^{\textcircled{P}}$-Pph21/22p acts as a phosphatase
V_7 :	Specific catalytic constants for dephosphorylation of Tip41p$^{\textcircled{P}}$ by PP2A1/2
V_8 :	Tap42p$^{\textcircled{P}}$-Sit4p forms an anti-phosphatase that protects phosphorylated proteins
V_9 :	Tap42p$^{\textcircled{P}}$-Sit4p is a phosphatase
V_{10}:	Sit4p is phosphorylated by Tor1/2p and dephosphorylated by PP2As
V_{11}:	Tap42p has two phosphorylation sites
V_{12}:	PP2A1/2 form with Sit4p and Pph21/22p bound to Tap42P and dephosphorylate it
V_{13}:	Tap42p$^{\textcircled{P}}$ bound to Sit4p or Pph21/22p can be dephosphorylated by PP2A1/2
V_{14}:	Specific constants for dephosphorylation of Tap42p$^{\textcircled{P}}$ by PP2A1 / PP2A2
V_{15}:	Monomeric Sit4p is an active phosphatase for Tip41p$^{\textcircled{P}}$
V_{16}:	Complex formation of Tap42p and Tip41p$^{\textcircled{P}}$
V_{17}:	Complex formation of Tap42p and Pph21/22p
V_{18}:	Complex formation of Tap42p and Sit4p

Table S1: **Variants of the mechanisms of TOR signalling.** Each of these variants represents an alternate mechanism for TOR signal transduction[1]. By combining more than one variant, several topological variants of the *core* topology can be generated.

	Description
1	Relative degree of Tap42p phosphorylation before and after the addition of rapamycin, in wild type[2].
2	Relative degree of Tap42p phosphorylation before and after the addition of rapamycin, in Δ*cdc55*/Δ*tpd3* mutants[2].
3	Tap42p-Tip41p complex formation before and after the addition of rapamycin, in wild type[3]
4	Tap42p-Tip41p complex formation before and after the addition of rapamycin, in Δ*sit4* mutants[3]
5	Tap42p-Sit4p complex formation before and after the addition of rapamycin, in wild type[3]
6	Tap42p-Sit4p complex formation before and after the addition of rapamycin, in Δ*tip41* mutants[3]
7	The amount of Tap42p-Pph21/22p in wild type present in complexes relative to the overall concentration[4,5]
8	The amount of Tap42p-Sit4p in wild type present in complexes relative to the overall concentration[4,5]
9	The amount of Sit4p-Sapp in wild type present in complexes relative to the overall concentration[4,5]
10	Tap42p-Pph21/22p concentration after the addition of rapamycin, in wild type[4]
11	Level of phosphorylated Tip41p$^{\textcircled{P}}$ upon addition of rapamycin, in wild type[1,3]

Table S2: **Experimental data on TOR signalling.** A brief description of the experimental measurements we used to compare the signalling behaviour of different model topologies to the canonical TOR pathway.

Expt.	Species	Strain	Rapamycin (nM)	δ	t (min)	Value (relative)
1	Tap42p$^{\textcircled{P}}$	WT	500	0.20	0	1.00
		WT	500	0.20	15	0.49
		WT	500	0.20	30	0.29
		WT	500	0.20	60	0.12
		WT	500	0.20	180	0.15
2	Tap42p$^{\textcircled{P}}$	Δ*cdc55*/Δ*tpd3*	500	0.20	0	2.60
		Δ*cdc55*/Δ*tpd3*	500	0.20	180	2.35
3	Tip41p-Tap42p	WT	109	0.20	0	1.00
		WT	109	0.20	30	5.43
		WT	109	0.20	180	5.43
4	Tip41p–Tap42p	Δsit4	109	0.20	0	1.02
		Δ*sit4*	109	0.20	30	1.38
		Δ*sit4*	109	0.20	180	1.38
5	Tap42p$^{\textcircled{P}}$-Sit4p	WT	109	0.20	0	1.00
		WT	109	0.20	30	0.40
		WT	109	0.20	60	0.40
6	Tap42p$^{\textcircled{P}}$-Sit4p	Δ*tip41*	109	0.20	0	1.12
		Δ*tip41*	109	0.20	30	0.82
		Δ*tip41*	109	0.20	60	0.82
7	Tap42p-Pph2122p/Tap42p(0)	WT	0	0.50	180	0.10
	Tap42p-Pph2122p/Pph2122p(0)	WT	0	1.00	180	0.02
8	Tap42p-Sit4p/Tap42p	WT	0	0.50	180	0.10
	Tap42p-Sit4p/Sit4p	WT	0	1.00	180	0.05
9	Sit4p-Sapp/Sit4p	WT	0	1.00	180	0.60
	Sit4p-Sapp/Sapp	WT	0	0.83	180	0.15
10	Tap42p-Pph2122p	WT	109	1.00	0	1.00
		WT	109	1.00	30	0.40
		WT	109	1.00	60	0.40
11	Tip41p$^{\textcircled{P}}$	WT	109	1.00	180	0.10

Table S3: **Experimental data points used for parameter estimation.** These data were obtained from multiple experiments[1–5], as detailed in Table S2 and ref. 1. WT=Wild-type.

References

[1] L. Kuepfer, M. Peter, U. Sauer and J. Stelling, *Nat Biotechnol*, 2007, **25**, 1001–1006.

[2] Y. Jiang and J. R. Broach, *EMBO J*, 1999, **18**, 2782–2792.

[3] E. Jacinto, B. Guo, K. T. Arndt, T. Schmelzle and M. N. Hall, *Mol Cell*, 2001, **8**, 1017–1026.

[4] C. J. Di Como and K. T. Arndt, *Genes Dev*, 1996, **10**, 1904–1916.

[5] M. M. Luke, F. D. Seta, C. J. D. Como, H. Sugimoto, R. Kobayashi and K. T. Arndt, *Mol Cell Biol*, 1996, **16**, 2744–2755.